

1 Title: Molecularly Imprinted Polymers for Cell Recognition

2

3 Stanislav Piletsky, Francesco Canfarotta, Alessandro Poma, Alessandra Maria Bossi*, Sergey
4 Piletsky

5

6 **Affiliations:**

7 Stanislav Piletsky - Imperial Coll, Dept Chem, London SW7 2AZ, England; e-mail:
8 stanislav.piletsky14@imperial.ac.uk

9 Francesco Canfarotta – MIP Diagnostics Ltd. Colworth Park, Sharnbrook, Bedford, MK44
10 1LQ England, e-mail: Francesco.Canfarotta@mip-dx.com

11 Alessandro Poma: UCL Eastman Dental Institute, 256 Gray's Inn Road, London, WC1X 8LD,
12 England; e-mail: a.poma@ucl.ac.uk

13 Alessandra Maria Bossi - Dept. of Biotechnol., University of Verona, Strada Le Grazie 15,
14 37134 Verona, Italy; website: <http://www.dbt.univr.it/?ent=persona&id=97>, email:
15 alessandramaria.bossi@univr.it

16 Sergey A. Piletsky, Chem. Dept., CSE, University of Leicester, LE1 7RH, England; website:
17 <https://www2.le.ac.uk/departments/chemistry/people/academic-staff/prof-sergey-a-piletsky>
18 e-mail: sp523@le.ac.uk

19

20 Correspondence: alessandramaria.bossi@univr.it (A.M. Bossi)

21

22

23 **Key words:** Molecularly imprinted polymers (MIPs), cell recognition, epitopes, targeted
24 delivery, sensors, stem cells

25

26 **Abstract:**

27 Since their conception fifty years ago, molecularly imprinted polymers (MIPs) have seen
28 extensive development both in terms of synthetic routes and applications. Perhaps the most
29 challenging target for molecular imprinting are cells. Though early work was based almost
30 entirely around microprinting methods, recent developments shifted towards epitope
31 imprinting to generate MIP nanoparticles. Simultaneously, the development of techniques such
32 as solid phase MIP synthesis have solved many historic issues of MIP production. This review
33 briefly describes various approaches used in cell imprinting with a focus on applications of the
34 created materials in imaging, drug delivery, diagnostics and tissue engineering.

35

36 **1 The drive to recognize and interact with cells**

37 The living functions in organisms arise from specific cell cross-talks which ultimately rely on
38 macromolecular interplays. Dysfunctional molecular interactions at cellular level are often
39 responsible for cell malfunctioning and the consequent onset of a disease [1]. Biomimetic tools
40 that explore molecular interactions have been used for cell imaging, improving drug delivery,
41 tissue engineering and diagnostics [2]. Design of such tools however is not easy due to complex
42 nature of molecular interactions and lack of affordable generic protocols suitable for the
43 development of supramolecular receptors with ordered system of functional groups that mimic
44 natural molecules. The present review focuses on molecularly imprinted polymers (MIPs), as
45 an alternative to biomimetics and biosimilars. We shall discuss here historical foundations and
46 the recent technology advancements for the preparation of MIPs suitable for cell recognition,
47 the frontier applications to cells and in cell biology, highlighting the achievements, the current
48 limitations and the future trends.

49

50 **2 Molecularly imprinted polymer: the concept.**

51 MIPs are recognition materials prepared by a template-assisted synthesis [3, 4]. The imprinting
52 process, schematized in Figure 1, consists in the polymerization of the monomers and the cross-
53 linker in the presence of a target molecule that acts as a template. Driven by thermodynamics
54 the template interacts with the monomers forming a pre-polymerization complex, stabilized by
55 molecular interactions, that is later “frozen” by polymerization. As a result, molecular
56 impressions of the template are stamped into the formed polymeric material creating specific
57 binding sites capable of recognition of template and its analogues.

58

Insert Figure 1.

59 MIPs are robust, and possess affinity and selectivity for the template comparable to that of
60 natural receptors. Small molecules, peptides, nucleic acids, proteins, cells and viruses have
61 been imprinted, confirming the versatility of the MIP approach [5-7]. With the recent progress
62 in development of MIP nanoparticles (nanoMIPs) [8,9], this technology became suitable for frontier
63 applications in the domain of life science and medicine.

64

65 **3 The development of whole-cell imprinted MIPs.**

66 Whilst the molecular imprinting of small molecules, peptides and even proteins is well-
67 established counting many examples in literature, patents and even commercial products (e.g.
68 SupelMIP® by Sigma-Aldrich, [www.sigmaaldrich.com/analytical-chromatography/sample-](http://www.sigmaaldrich.com/analytical-chromatography/sample-preparation/spe/supelmip.html)
69 [preparation/spe/supelmip.html](http://www.sigmaaldrich.com/analytical-chromatography/sample-preparation/spe/supelmip.html)), the holy grail of MIP technology is the imprinting of complex
70 template structures such as whole cells. These MIPs would have a broad range of applications,
71 including use in environmental and clinical assays, targeted therapeutics and imaging, cell
72 separation and tissue culturing. Over the past two decades much effort has been put towards
73 the successful achievement of this goal with successful examples such as cell-imprinting using
74 stamping of the whole cells [7]. The proof of concept was performed by Vulfson and colleagues
75 in 1996 [10,11]. It involved cell lithography for preparing polymers with affinity for bacteria.
76 Since then, micro-contact stamping has seen extensively development, along with alternative
77 strategies such as the preparation of MIPs from self-assembling silica nanoparticles, and the
78 use of cell epitopes in place of whole cells.

79

80 **2 Micro-contact stamping**

81 Micro-contact stamping, otherwise referred to as microprinting, is the most frequently explored
82 technique to generating MIPs using whole cells as templates [7]. It involves deposition of the

83 target cells on a flat solid support layer and then topping them with monomers or a soft polymer,
84 such as pre-polymerised polyurethane (PU). The polymer is then cured, sandwiching cells
85 between the support layer and the formed polymer (Figure 2). Whole-cell MIPs exhibited
86 shape, size and functional selectivity for the cell templates [11, 12]. Key example of cell-
87 recognizing MIPs is found in using imprinted poly-vinylpyrrolidone (PVP) for the selection
88 of erythrocyte subtypes [13]. Developed MIPs have shown outstanding selectivity towards
89 erythrocyte subgroups A1 and A2, despite both types exposing the same antigens on the
90 surface, differing solely in the density of glycolipids on the respective cells. These results
91 permitted to conclude that in contrast to antibodies, whose recognition ability relies on the
92 presence of a defined antigen on the cell surface, MIPs instead are able to interact with the
93 entire cell surface showing sensitivity to quantitative differences in surface chemistry [14]. A
94 broad range of targets and materials have already been imprinted using this approach, including
95 bacteria, mammalian cells and yeast with key examples reported in Table 1 [15, 16].

96 Insert Figure 2.

97 Microcontact stamping was successfully exploited for cell recognition, cell selection and
98 sensing purposes (Table 1). Microcontact stamping provided also surfaces suitable for
99 controlled cell growth. Interestingly the comparison of cells grown on flat and imprinted
100 surfaces showed that MIP surfaces promoted higher expression levels in adhesion proteins,
101 confirming the MIP substrate elicits biochemical response in the growing cell [17-19].

102 Microcontact printing can be performed using both, organic and inorganic polymers.
103 Commercial ready-to-use organic polymers such as polystyrene (PS), polyacrylate,
104 polyvinylpyrrolidone (PVP), polyacrylamide, PU and Epon1002F were used to generate
105 imprinted surfaces for *Bacillus cereus* [20]. The best performance was achieved with PU and
106 Epon1002F. This is an important result, as it allows replacing self-synthesised polymers with

107 well characterised commercial materials, with the outcome to enable use of this technique by
108 non-specialists in polymer synthesis.

109 More recently, Dulay and colleagues assessed the ability of a polydimethylsiloxane (PDMS)
110 layer created by micro-contact stamping of bacterial cells to distinguish between living and
111 inactivated cells [14]. These polymers showed significantly higher affinity for inactivated cells
112 prepared using the same technique as was used for polymer imprinting [14,17]. But, due to the
113 synthetic limitations of PDMS, authors moved to organosiloxane polymers made by sol-gel
114 chemistry. The broad selection of available silanes allowed to benefit from a plethora of
115 functionalities whilst retaining optical transparency and mechanical resistance [21]. Although
116 the mechanical stability of inorganic materials is usually higher than their organic counterparts,
117 it is important to consider the mechanical stress which the cells undergo during the stamping
118 procedure, might be damaging more delicate targets, such as human cells.

119 A superior strategy in cell imprinting lies in generating a polymer layer using cells as a
120 template, and then using this as a mould to generate a second polymer layer. This layer can
121 then act as a “master mould” that can be used to use as a template instead of bacteria. This may
122 improve the ease, reproducibility and safety of making imprinted polymer layers, as no living
123 bacteria are needed after the first imprint [18].

124

125 *Imprinting of sections of cell membranes* - Cell recognition can also be achieved by imprinting
126 sections of cell membrane. It is known that charged proteins exposed on the cell membrane
127 have a key role in adhesion, proliferation, interaction and localization of the cell. Bao and
128 colleagues reported a novel method to produce bacteria-imprinted polymers by exploiting the
129 bacterial surface-charge heterogeneity using charged methacrylate ethyl trimethyl ammonium
130 chloride and 3-dimethyl (methacryloyloxyethyl) ammonium propane sulfonate fixed in

131 polymer network by surface-initiated atom transfer radical polymerisation (ATRP) [22]. The
132 charge distribution on the imprinted cavities complemented the charge distribution of the
133 bacteria surface, allowing for stronger electrostatic-mediated recognition. Borovicka and
134 colleagues fabricated “colloid antibodies” by coating microbial cells with a silica shell that was
135 subsequently fragmented to create complementary shell fragments [23,24]. Authors
136 demonstrated that the recognition is mediated by the size and shape of the imprints but also
137 electrostatic interactions and the surface charge of the microbial cells.

138 A sophisticated whole-cell imprinting approach was developed by Alexander and colleagues,
139 who exploited bacterial redox systems to induce copper-mediated ATRP of cationic 2-
140 (methacryloyloxy)-N,N,N-trimethylethanaminium chloride and zwitterionic 2-(N-3-
141 sulphopropyl-N, N-dimethyl ammonium) ethyl methacrylate at the surface of *E. coli* and *P.*
142 *aeruginosa* cells, thus generating polymers directly *in situ* at the surface of the microorganisms
143 [25]. The cells also doubled as a solid-phase to isolate high-affinity from low-affinity polymer
144 products, similar to the technique pioneered by Piletsky and colleagues [8, 26–27]. A “click”
145 chemistry reaction was used to attach fluorescent reporters on the polymers, to simultaneously
146 bind and visualise the pathogens (Figure 3).

147

148 Insert Figure 3.

149

150 **3. Epitope imprinting**

151 The whole-cell imprinting approach produce a shape-recognition material, that might not be
152 optimal when the goal to achieve is the recognition of a specific type of human cell, such as
153 the ability to differentiate or locate cancer cells in a tissue or in an organ. Given the high
154 plasticity of mammalian cells, the sole shape recognition is not always offering the level of

155 discrimination required for success. Moreover, MIPs intended for cell recognition *in vivo*
156 should have the size of natural macromolecules (nanometers), so to be suitable for circulation
157 within vessels, within the lymphatic system and for the intracellular space diffusion, whereas
158 the imprint of a whole cell inevitably results in micrometer size. For all these reasons,
159 alternative imprinting approaches had to be proposed. In the case, attention should focus on
160 particular molecular components present on the cell surface such as proteins, lipids, saccharides
161 and their derivatives.

162 *Saccharides* - When targeting the glycomoieties typically present on the cell surface, the
163 imprinting process was performed by stamping portions of glyco-architecture, in a process
164 analogous to the epitope imprinting [28]. Monosaccharides such as sialic acid and mannose
165 have been used most frequently as representative targets [29–33]. In another example Kinoshita
166 and colleagues have created core-shell imprinted gold nanoparticles bearing thermo-responsive
167 *N*-isopropylacrylamide (NIPAm) imprinted with *E. Coli* O157 lipopolysaccharide [34]. The
168 target bacteria bound to the nanoparticles with excellent selectivity (>15) against other types
169 of *E. coli*. NanoMIPs, prepared using a solid-phase approach with immobilised trisaccharide
170 of the blood type B-antigen, were able to distinguish between erythrocytes of different blood
171 types [35]. Similarly, MIPs made for glycans were able to differentiate between different types
172 of cancer cells [36].

173 *Proteins* - Proteins of cell membranes are obvious targets for cell imprinting. Imprinting of
174 entire proteins or corresponding peptide epitopes is a well-established technique [28,37]. For
175 example, the whole protein was imprinted in the preparation of a fibronectin (FN)-imprinted
176 polysiloxane membrane, made using silanes as functional monomers and calcium alginate
177 hydrogel membrane as the substrate. The FN-imprinted polysiloxane membrane provided
178 improved cell adhesion and favourable cell growth for mouse fibroblasts (L929) [38].
179 Unfortunately, most membrane proteins are prohibitively expensive and for this reason are

180 rarely used as templates in molecular imprinting. A much more exploitable concept is the
181 imprinting of a small peptide sequence - epitope that is characteristic for a particular protein
182 and exposed on its surface. Finding such epitopes due to extreme complexity of the proteome,
183 is a difficult task. A short summary provides an outline of the strategy currently used in the
184 rational selection of epitopes for molecular imprinting (Box I and II).

185 A recent example of epitope imprinting describes the use of the peptide arginylglycylaspartic
186 acid (RGD) with well-known cell-adhesive function. An RGD-imprinted surface was
187 successfully designed to anchor RGD and consequently cells [39]. In another example, the
188 progastrin-releasing peptide was used as template to prepare molecular imprinting sites of
189 zeolite-chitosan-TiO₂ microspheres for dot-blot immunoassays with multiple native antigens
190 for rapid serodiagnosis of human lung cancer [40].

191 An epitope imprinting approach was exploited to generate amoxicillin delivery systems aimed
192 at *Helicobacter pylori* [41,42]. In this system, the primary template was a modified epitope
193 sequence of Lpp20, a membrane lipoprotein specific to *H. pylori*. The modification exploited
194 the conjugation of a lipophilic chain to guarantee the presence of the template at the surface of
195 the nanoparticles during the inverse microemulsion polymerisation method.

196 Similarly, cancer cells overexpressing epidermal growth factor receptor (EGFR) have been
197 successfully targeted by imprinting NIPAm-based MIPs with an epitope of EGFR [43]. The
198 resultant MIPs were able to differentiate between cells with differing levels of EGFR
199 expression. These MIPs were prepared by first immobilising the template peptide on glass
200 beads prior to polymerisation. Using this solid-phase approach, it was possible to remove low-
201 affinity polymers and monomers with a low-temperature washing step, and easily separate high
202 affinity MIPs from template molecules (Figure 4).

203

204

Insert Figure 4.

205

206 To conclude – two approaches continue to dominate cell imprinting – microprinting and
207 epitope imprinting. A range of organic and inorganic polymers were employed to imprint
208 bacterial and mammal cells successfully. While microprinting is perfectly suited for producing
209 cell-specific surfaces, epitope imprinting can be used to produce nanoMIPs capable of
210 addressing cell targets *in vivo*.

211

212 **4 Applications**

213 *Cell concentration and separation*– Most successful examples of the use of cell-imprinted
214 MIPs in separation are related to capturing and separating bacteria. The possibility of
215 separating different strains of bacteria by electrophoresis was demonstrated in 2006 [44].
216 Imprinted gel granules were synthesized from acrylamide and N,N'-methylenebisacrylamide
217 in the presence of *E. coli* as a template. The electrophoretic migration of the gels was affected
218 by the presence of the template, showing good discrimination between *E. coli* MRE-600, and
219 *E. coli* BL21. Specific capturing of *Deinococcus radiodurans*, *E. coli*, *Sphaerotilus natans* and
220 *Bacillus subtilis* by imprinted films was achieved by Cohen and colleagues [45]. Surface
221 imprinted PU films were used for selective capturing of methanotrophs from paddy soil [46].
222 The use of virulent bacteria during the production of the cell-imprinted polymer thin films and
223 the cell-capture process bears an obvious and persistent risk of infection, which could be a
224 major hurdle for the implementation of this method. A successful attempt was made to remove
225 the potential biohazard risk by using inactivated bacteria, when poly(dimethylsiloxane) films
226 were imprinted with inactivated *M. smegmatis* [14].

227 Apart from bacteria, MIPs were used for spore capture and concentration within an integrated
228 biological detection system for *Bacillus anthracis* [47]. The binding assay showed strong
229 spore-binding capability and a robust imprinting effect that accounted for 25% additional
230 binding over non-imprinted controls. This process was rapid, taking only 30 minutes.

231 In a different example, cell adhesion was improved by the imprinting of FN and cell-adhesive
232 peptide Arg-Gly-Asp-Ser [48,49]. Template-enhanced adhesion of fibroblasts, MC3T3-E1,
233 and L929 cells was observed after 24 hours (Figure 5).

234

235  Insert Figure 5.

236

237 *Tissue engineering* - Numerous studies have previously indicated that stem cell fate is regulated
238 by a combination of intrinsic (e.g., specific transcription factors) and extrinsic mechanisms
239 invoked by the local microenvironment [50,51]. Stem cells sense different mechanical cues
240 that guide rearrangement of adhesion proteins and the cytoskeleton, which in due course affect
241 intracellular processes [52]. The predictive design of tissue scaffolds is difficult due to limited
242 understanding of microenvironment patterns that guide cell differentiation. Molecular
243 imprinting may offer a solution to this problem.

244 In one study, tissue-specific substrates were prepared by imprinting mature and
245 dedifferentiated chondrocytes. Rabbit adipose derived mesenchymal stem cells seeded on cell-
246 imprinted substrates were driven to adopt the specific characteristics of the cell types used as
247 templates for cell imprinting [53]. Besides residual cellular fragments presented on the template
248 surface, the imprinted topography of the templates played a role in stem cells differentiation.
249 In a similar study, mature human keratinocyte cells were used in the imprinting of PDMS.
250 Human adipose-derived stem cells (ADSCs) seeded on cell imprinted substrates were driven

251 to adopt the specific shape and characteristics of keratinocytes [54]. The observed morphology
252 of the ADSCs grown on the keratinocyte casts was noticeably different from that of stem cells
253 cultivated on the stem cell imprinted substrates. Authors speculate that mechanical deformation
254 caused by cell-imprint interaction may induce transduction by affecting the chromatin
255 arrangement inside the stem cell nucleus. ADSCs, semifibroblasts and tenocytes were
256 differentiated, redifferentiated and transdifferentiated, respectively, into chondrocytes after
257 being cultured for 2 weeks onto chondrocyte-imprinted PDMS substrates [55]. A similar effect
258 was also observed when ADSCs were cultured on keratinocytes-imprinted substrates [54] or
259 on chondrocytes or fibroblasts-imprinted substrates [53]. Although the aim of these works was
260 to develop an efficient and cheap approach for regenerative medicine and wound healing, it is
261 likely that MIP-guided cell differentiation can be used on a large scale for growing more
262 complex tissues, and potentially whole organs.

263 The advantage of using molecular imprinting in guiding cell differentiation lies in the relatively
264 simple procedure for creating topographical cell fingerprints for directed tissue growth. In
265 clinical usage, an opportunity exists for the use of MIPs in the enrichment of cell populations,
266 for example, separation of leukocytes by aphaeresis or enrichment of haematopoietic stem
267 cells, and aiding repopulation of the immune system, for example, in multiple sclerosis patients
268 who have undergone immunoablation treatment [56–58]. In these applications, MIPs have to
269 compete with antibody-binding methods such as fluorescence-activated and magnetic-
270 activated cell sorting [59]. It should be noted that in most cases the selective recognition of
271 nanoMIPs is at least in line with that of the antibody [60], moreover the possibility to produce
272 fluorescent nanoMIPs and/or core-shell magnetic nanoMIPs is well recorded [61], therefore
273 the MIP technology is sufficiently mature for the challenge.

274 *Drug delivery* - There is a current trend in pharmacology represented by the increasing number
275 of FDA-approved nanoparticle formulations, amounting to ~50 in 2017 [62]. Currently, several

276 types of nanoparticle-based drug carriers are available on the market. They are based on solid
277 dispersion (Gris-PEG, Sandimmune, Intelence etc.), self-emulsifying drug delivery systems
278 (Neoral®, Agenerase, Aptivus etc.) or nanocrystals (NanoCrystal®, Rapamune, Megace® ES)
279 [63]. The polymer architecture of nanoparticles dictates drug loading effectiveness, drug-
280 release rate and biodistribution [64]. Nanoparticles (NPs) smaller than 8 nm are cleared rapidly
281 from the blood stream by the renal system and NPs larger than 200 nm are sequestered by the
282 mononuclear phagocytic system in the liver and spleen [65,66]. NanoMIPs represent an
283 entirely new compound class which can now be deployed to address both extracellular protein
284 targets (as an alternative to biological antibodies), and potentially to currently intractable
285 intracellular proteins [67]. Potentially nanoMIPs can assist with increasing a drug's half-life
286 within the body, increasing drug payload, facilitating targeted drug delivery, improving drug
287 permeability through cell membranes and offering the possibility of oral delivery.

288

289 One particularly important subject in NP research is the oral delivery of macromolecules. The
290 main mechanism for NPs transport is adsorptive endocytosis [68]. Summarizing numerous
291 absorption studies, there seems to be an agreement that the optimum size of NPs suitable for
292 drug delivery via oral route is 10-100 nm [69]. The extent of systemic appearance of this type
293 of NP after gastrointestinal absorption has been reported as 10-15% [70]. NanoMIPs, in
294 contrast to antibodies and aptamers, are capable of penetrating cell membranes by endocytosis,
295 and even reaching nuclei [67,71]. The same mechanism is used for oral delivery of drugs
296 assisted by nanoMIPs. In one such example nanoMIPs were made by precipitation
297 polymerization and used for the oral delivery of insulin through a transmucosal oral route
298 (Figure 6) [72].

299

Insert Figure 6.

300

301 Recently, Piletsky and colleagues have compared intravenous and oral delivery of nanoMIPs
302 and their impact on the clearance of nanoparticles through kidney and bile. Interestingly, the
303 nanoMIPs were successfully excreted in both urine and faeces (Figure 7). Oral administration
304 showed an increased level of faecal excretion, in line with other clearance data for NPs through
305 the hepatic route. No particles were detected one week after administration.

306

307

Insert Figure 7.

308

309 Due to their size and the large number of functional groups available for
310 entrapment/conjugation of drug molecules, nanoMIPs have great potential as drug carriers.
311 Most papers published on this topic describe entrapping drug molecules in the bulk of
312 polymers. The delivered/released quantity of drugs varies from 0.5-180 $\mu\text{g}/\text{mg}$ of
313 nanoparticles, depending on the drug type and synthetic protocol used in the nanoMIPs
314 preparation [71,73–75]. The imprinting process ensures a 2-3 time increase in the quantity of
315 entrapped drugs as compared to non-imprinted particles [75]. The half-time drug release in
316 these experiments varied from 2-20 hours based on the drugs polarity and its affinity to the
317 polymer carrier. This is significantly shorter than the circulation time of synthetic particles
318 demonstrated in clinical trials, which is under 12 days [76]. The average results obtained for
319 nanoMIPs circulation in the body are 7 days which is an improvement as compared with
320 circulation of small drug molecules [77].

321

322 Targeted drug delivery originates from MIPs ability to interact specifically with cell receptors.
323 Most therapeutic agents (90% or more) will inevitably be concentrated in the
324 reticuloendothelial organs such as the liver and spleen due to clearance by mononuclear
325 phagocytes [78]. Active targeting is being explored as a method to achieve spatial localization

326 of drugs in diseased organs while eliminating off-target adverse effects in normal tissue. The
327 ligands used to modify nanoparticles include antibodies, their fragments, proteins, peptides and
328 aptamers [79]. NanoMIPs can also be decorated with specific ligands to achieve a targeting
329 effect. Thus nanoMIPs containing folic acid showed a greater amount of intracellular uptake
330 in folate receptor-positive cancer cells (MDA-MB-231 cells) in comparison with the non-folate
331 nanoparticles and free paclitaxel, with half maximal inhibitory concentrations (IC₅₀) of
332 4.9 ± 0.9 , 7.4 ± 0.5 and 32.8 ± 3.8 nM, respectively [74]. Sialic acid-coated nanoMIPs with S-
333 nitrosothiols were used for nitric oxide-release as chemotherapy agents [80]. Specific targeting
334 of cancer cells was achieved by nanoMIPs imprinted with EGFR epitope [81]. In a similar
335 way, senescent cells were targeted by dasatinib-bearing nanoMIPs imprinted with epitope of
336 senescent markers B2M [82]. NanoMIPs loaded with drugs were able to specifically kill
337 senescent cells, showing significantly greater level of binding within organs of older animals.
338 Targeted delivery can be achieved using external factors such as magnetic field [77]. In this
339 work, nanoMIPs with magnetic cores were prepared via co-precipitation polymerization in the
340 presence of olanzapine as a template, and used for magnetic field-guided drug delivery of
341 olanzapine to rat brains.

342

343 So far, most examples related to drug delivery describe drug loading through the binding to
344 imprinted sites in the polymer matrix. This may not be the most desirable way, as the produced
345 nanoparticles typically release their drug cargo too quickly, within 4-7 hours. The covalent
346 attachment of drugs through cleavable linkers would be preferred. This approach follows
347 similar trends with the conjugation of drugs with antibodies [83–85].

348

349 In a rare example, nanoMIPs themselves were used as a drug [86]. In this work, nanoMIPs,
350 imprinted with the quorum signalling peptide SNGLDVGKAD, prevented the translocation of
351 pneumococci from lungs to blood and improved the survival rate of infected mice.

352

353 In a very interesting example of a theranostic application, amphiphilic lipopolysaccharides,
354 derived from *Pseudomonas aeruginosa*, were used as a template in the preparation of
355 nanoMIPs by the inverse emulsion method [87]. Fluorescent nanoMIPs, labelled with IR-783,
356 showed selective recognition of target bacteria in keratitis and meningitis models (Figure 8).
357 *P. aeruginosa*-targeted nanoMIPs encapsulated with a photosensitizer (methylene blue) were
358 used also for *in vitro* photodynamic therapy. Compared to non-imprinted NPs, an almost two
359 order of magnitude difference in cell counting was noted, indicating the higher efficacy of
360 nanoMIPs against bacteria after laser exposure. The nanoMIPs formulation was very stable,
361 showing similar performance after six months storage.

362

363 Insert Figure 8

364

365 There are a number of issues to be resolved and questions to answer before practical application
366 of nanoMIPs in drug delivery can be considered. Among these are:

- 367 • How safe are nanoMIPs?
- 368 • Should nanoMIPs be biodegradable?
- 369 • How do nanoMIPs properties influence their biodistribution and clearance?
- 370 • What is the best way to conjugate drugs to nanoMIPs?
- 371 • How can nanoMIPs be produced on a large scale and in accordance with quality-control
372 guidelines such as Good Laboratory Practice?

373

374 So far nanoMIPs were tested mainly *in vitro*. Cell viability tests (NIH-3T3) using human
375 embryonic kidney (HEK293) suggested that the developed material did not present any
376 detectable cytotoxicity at $<100 \mu\text{g mL}^{-1}$ nanoMIP concentrations [71,77,88]. Limited *in vivo*
377 tests also showed that nanoMIPs had no visible impact on the hepatocytes and the structure of
378 the kidney. No sign of toxicity was found, no body weight changes or clinical symptoms (i.e.
379 diarrhea, fever) were found 14 days after the experiment [72].

380

381 The answer to the question of whether MIP formulations should be biodegradable is not
382 straightforward. Potentially, biodegradable nanoMIPs might have simplified clearance process.
383 However, the byproducts of polymer degradation might be more toxic than the nanoparticles.
384 Monomers such as methacrylic acid, methyl methacrylate and ethylene glycol dimethacrylate
385 are biocompatible and non-toxic [89,90]. The same is not true for some other monomers such
386 as acrylamide [91]. The examples shown in this paper, as well as many other relevant examples
387 from literature, imply that non-degradable polymers might be safer for use in medical devices
388 and drug delivery [92,93]. Besides the residual monomers, other toxic impurities can be present
389 in a plastic product, including oligomers, low molecular weight polymer fragments, catalyst
390 remnants and surfactants [94]. It is therefore essential to ensure the complete removal of non-
391 polymerised components from MIPs formulation.

392

393 Besides the complications in the experimental design of nanoparticles, there are multiple
394 challenges in the manufacturing, regulation, and approval of nanoparticles for clinical use. The
395 majority of protocols describing the synthesis of nanoMIPs cannot be easily adapted to large-
396 scale manufacturing. A major breakthrough was therefore the combination of nanoMIP
397 synthesis with an affinity separation step into a single procedure, using an immobilised
398 template for MIP formation [95]. The resulting process allowed the construction of the first

399 prototype automatic nanoMIP synthesiser [8]. The process of MIP synthesis using the
400 automated reactor is shown schematically in Figure 3. This approach represents the state-of-
401 the-art in nanoMIP synthesis: not only can soluble particles with a well-defined size (30-100
402 nm) and a narrow size distribution be produced in a matter of one hour, but they possess
403 nanomolar dissociation constants for their respective targets, there is no residual template
404 present and the immobilised template can be re-used. This automated process overcomes all of
405 the historic drawbacks of bulk MIPs, and raises the exciting possibility of deploying nanoMIPs
406 in therapeutic applications. Despite this success, bringing manufacturing protocol to
407 compliance with Good Laboratory Practice and Good Manufacturing Practice, as well as
408 passing FDA Investigational New Drug trials, will be challenging.

409

410 *Imaging* - In many ways, drug delivery and imaging are connected. Both applications should
411 address safety issues and the issue of targeted delivery to specific cells and organs. For imaging
412 applications, nanoMIPs should have fluorescent, magnetic or positron-emitting tags. So far
413 only fluorescent labels were used in combination with nanoMIPs, including pyrene, fluorescein
414 and rhodamine derivatives [29,96], quantum dots [97] and carbon dots [33]. In one study, two
415 differently colored nanoMIPs were imprinted with D-glucuronic acid and N-acetylneuraminic
416 acid. Both MIPs were found to be highly selective towards their target monosaccharides, as no
417 cross-reactivity was observed with other sugars present on the cell surface [32]. Fluorescently-
418 labeled nanoMIPs were used for multiplex imaging of fixed and living human keratinocytes,
419 to localize hyaluronan and sialylation sites (Figure 9). Monodispersed 400 nm sized particles
420 bound their targets located in the extracellular region. In contrast, 125 nm particles were able
421 to stain the intracellular and pericellular regions as well.

422

Insert Figure 9.

423

424 In a similar work, fluorescent nanoMIPs were imprinted with sialic acid and used for the
425 imaging of cancer cells [31]. These nanoMIPs exhibited selective staining for DU 145 cancer
426 cells and did not enter HeLa cells even after long incubation times. In a previously mentioned
427 work fluorescent nanoMIPs were imprinted with a linear epitope of EGFR and used in confocal
428 microscopy [81]. A strong fluorescent signal was detected from the MIPs in MDA-MB-468
429 cells over-expressing EGFR, whereas almost no signal was observed in MDA-231 or SKBR3
430 cells. These results show that nanoMIPs can potentially be used as a cell imaging tool against
431 difficult targets such as membrane proteins.

432
433 Very few papers actually describe the use of nanoMIPs *in vivo*. In a rare example, nanoMIPs
434 were imprinted with human VEGF and coupled with quantum dots (QDs) for cancer imaging
435 [98]. The composite nanoparticles exhibited specific binding toward human melanoma cell
436 xenografts, overexpressing hVEGF, in zebrafish embryos. In another work, fluorescein-
437 labelled nanoMIPs, imprinted with senescence membrane marker B2M, were used for the
438 selective targeting of senescent cells [82]. NanoMIPs were able to detect senescent cells in
439 aged mice without eliciting any apparent toxicity (Figure 10).

440
441 Overall nanoMIPs are promising materials which can be considered for advancing imaging, in
442 particular when antibodies are less desirable due to their immunogenicity or long production
443 time. Moreover, one of the main limitations associated to the state of art in imaging techniques
444 is the detection limits of fluorescent antibodies, currently set to antigens expressed on the target
445 cell more than 1000 times/cell, whereas key inflammatory and cancer markers, such as
446 interleukins, are often present in just few hundreds of copies on the cell membrane, therefore
447 escaping the current detection limits [99]. Yet the nanoMIPs, given their larger dimensions
448 (10-400 nm), contain significant number of fluorophores *per* nanoparticle, surpassing the

449 aforementioned limitations, without need for secondary bindings or amplifying catalytic
450 events. Despite holding great promises, nanoMIP-based bioimaging is still in its infancy and
451 more work is required before it can be considered for practical applications. The research focus
452 in this area should shift from fluorescence to MRI and PET imaging. It is critically important
453 that safety issues are addressed and manufacturing problems solved for this technology to
454 advance.

455

456 Insert Figure 10.

457

458 *Sensing* - In diagnostics cell-imprinted MIPs are used almost entirely for the detection of
459 microorganisms. Currently, laboratory-based biochemical methods for microorganism analysis
460 are performed by means of standard antibody assays and polymerase chain reaction [100]. Cell
461 culture still remains a standard technique for identifying bacterial species; however, it usually
462 requires 24–48 hours, depending on the growth speed of the target bacterium [101]. These
463 methods generally require a high level of technical skill, and complex sample preparation.
464 There is therefore an industry-driven requirement to design novel, rapid and reliable analytical
465 detection methods for microorganisms.

466 A QCM sensor platform was developed for the detection of *Escherichia coli*, *Bacillus Cereus*,
467 *Pseudomonas aeruginosa*, *Bacillus subtilis* and *Staphylococcus aureus* [101-103]. Imprinted
468 PPy and PU were generated directly on sensor surface. The QCM device allowed detection of
469 microorganisms at concentrations of 1.4×10^8 cells/mL within 2-3 minutes. Overall, the QCM
470 sensors have shown similar sensitivity to SPR, afforded 10 regeneration cycles and worked for
471 at least 3 months [104]. In an example of practical application, PU-based QCM sensor was
472 used to follow growth processes of *Escherichia coli* and *Saccharomyces cerevisiae* in a

473 bioreactor [105,106]. The sensor was able to identify different stages of the cell cycle, with a
474 LoD of 1.6×10^8 cells/mL.

475

476 Electrochemical sensors based on conducting MIP materials, such as electropolymerised 3-
477 aminophenol and 3-aminophenylboronic acid, were used for the detection of *Staphylococcus*
478 *aureus* and *Staphylococcus epidermidis* [107,108]. Cyclic voltammetry and electrochemical
479 impedance spectroscopy in the presence of redox probes were explored for specific detection
480 of the target bacteria at 10^3 – 10^7 cfu/mL concentrations. Imprinted PPy/poly(3-
481 methylthiophene) was used in impedance detection of *Bacillus subtilis* endospores at 10^4 - 10^7
482 cfu/mL concentration [109]. Surface-imprinted polydopamine was used for yeast sensing,
483 allowing a LoD of 50 cfu/mL with excellent selectivity against smaller *Vibrio alginolyticus*,
484 *Escherichia coli* and *Staphylococcus aureus* [110]. A microprinting method was used to
485 develop a capacitive sensor for *E. Coli* with a LoD of 70 cfu/mL [111]. This sensor was able
486 to detect the target in river water. Electropolymerised 3-aminophenylboronic acid was used to
487 create a sensor for *Staphylococcus epidermidis* using electrochemical impedance spectroscopy
488 [108]. The same type of transducer was exploited by Qi and colleagues to create an imprinted
489 sensor for sulfate-reducing bacteria on chitosan doped with reduced graphene sheets. The
490 sensor performed in the range of 1×10^4 - 1×10^8 cfu/mL [112]. NanoMIPs were synthesized
491 using a sol–gel method with cerium dioxide nanoparticles in the presence of *Staphylococcus*
492 *aureus* on the surface of an indium tin oxide [113]. This assay was used to detect
493 *Staphylococcus aureus* at 10^4 - 10^5 cfu/mL concentrations.

494

495 An electrochemiluminescence biosensor was developed for the quantitative detection of
496 *Escherichia coli* O157:H7 based on a polydopamine-imprinted polymer [114]. However, in
497 this work MIPs were only used for capturing of bacteria, and the electrochemiluminiscent

498 detection was achieved using a polyclonal antibody labeled with nitrogen-doped graphene
499 quantum dots. The LoD was very low, at 8 cfu/mL.

500

501 Thermal wave analysis was used for a bacterial identification assay involving PU imprinted
502 with nine different bacterial targets [115]. The limit of selectivity of the sensor was tested in a
503 mixed bacterial solution in the presence of a 99-fold excess of competitor species. This
504 platform was able to detect bacteria at 3×10^4 cfu/mL in spiked urine.

505

506 In a rare example of a non-bacteria imprinting, the microprinting approach has been exploited
507 to produce sensors capable of detecting breast-cancer cells (MCF-7 or ZR-75-1 cells),
508 immortalised T-lymphocytes associated with leukaemia (Jurkat cells) and healthy peripheral
509 blood mononuclear cells [116–118].

510 In most of these examples, imprinted films were prepared by stamp imprinting or by
511 electropolymerisation. The main problem of these approaches lies in their poor reproducibility
512 and inefficiency in mass manufacturing of sensor devices, due to the use of live bacteria as
513 templates. There is also danger in using pathogenic bacteria as a template in sensor production.
514 The solution to these problems was found in anti-idiotypic imprinting using PDMS master
515 stamps with “plastic copies” of natural cells [119]. Sensitive layers created this way were
516 capable of the differentiation between *Saccharomyces cerevisiae* and *Saccharomyces bayanus*
517 and detect erythrocytes in ABO blood group typing [45]. In addition to the advantage of
518 improved reproducibility and standardization, such layers on mass-sensitive devices featured
519 the same selectivity and sensitivity as MIPs generated using native cells.

520

521 **5 Conclusion**

522 Molecular imprinting represents the most generic, versatile, scalable and cost-effective
523 approach to the creation of synthetic molecular receptors for small molecules and cells to date.
524 The approaches reported so far span from whole cell imprinting to targeting specific and
525 distinctive cell-surface components and the many recent developments in the synthesis of
526 MIPs, such as the use of a solid phase approach and contact printing permit, for the first time,
527 a reliable supply of soluble synthetic nanoparticles and polymer coatings with pre-determined
528 molecular recognition properties, sub-nanomolar affinities, defined size and surface chemistry
529 available for life science applications, drug delivery, imaging and diagnostics. Indeed targeting
530 specific cells, such as human cancer cells, or pathogenic bacteria, by utilizing nanoMIPs would
531 contribute to revolutionize clinical practice enabling personalized medicine [33, 40, 98].
532 Summarized in the Outstanding Questions are many crucial open challenges that should be
533 addressed. Worth mentioning is the challenge of producing nanoMIP architectures suitable to
534 translating MIP-mediated cell-recognition from the passive stage of binding to its defined
535 target, to the active intervention in the cell biology process. To accomplish this important step,
536 the integrated design of MIPs with multi-functions is expected, gathering in a single nanoMIP
537 particle ability to activate or silence biochemical pathways [37,120]. The success in this area
538 will result and in new paradigms for MIP applications both complementing existing therapeutic
539 and diagnostic techniques and opening doors to *in situ* programmed nanomachines for
540 precision medicine interventions and tissue regeneration.

541

542

543 **7. References**

544

- 545 1 Uversky, V.N. (2018) Chapter Four - Intrinsic Disorder, Protein–Protein Interactions,
546 and Disease. *Adv. Prot. Chem. Struct. Biology* 110, 85-121

- 547 2 Milroy, L-G. *et al.* (2014) Modulators of Protein–Protein Interactions. *Chem. Rev.* 114,
548 4695–4748
- 549 3 Arshady, R. and Mosbach, K. (1981) Synthesis of substrate-selective polymers by
550 host-guest polymerization. *Macromol. Chem. Phys.* 182, 687-692
- 551 4 Wulff, G. and Sarhan, A. (1972) The use of polymers with enzyme-analogous
552 structures for the resolution of racemates. *Angew. Chemie - Int. Ed.* 11, 341
- 553 5 Pan, J. *et al.* (2018) Molecularly imprinted polymers as receptor mimics for selective
554 cell recognition. *Chem. Soc. Rev.* 47, 5574-5587
- 555 6 Bossi, A *et al.* (2007) Molecularly imprinted polymers for the recognition of proteins:
556 The state of the art. *Biosens. Bioelectron.* 22, 1131-1137
- 557 7 Dickert, F.L. and Hayden, O. (2002) Bioimprinting of polymers and sol-gel phases.
558 Selective detection of yeasts with imprinted polymers. *Anal. Chem.* 74, 1302–1306
- 559 8 Poma, A. *et al.* (2013) Solid-Phase Synthesis of Molecularly Imprinted Polymer
560 Nanoparticles with a Reusable Template-"Plastic Antibodies". *Adv. Funct. Mater.* 23,
561 2821–2827
- 562 9 Hoshino, Y. *et al.* (2008) Peptide Imprinted Polymer Nanoparticles: A Plastic
563 Antibody. *J. Am. Chem. Soc.* 130, 15242-15243
- 564 10 Aherne, A. *et al.* (1996) Bacteria-mediated lithography of polymer surfaces. *J. Am.*
565 *Chem. Soc.* 118, 8771–8772
- 566 11 Alexander, C. and Vulfson, E.N. (1997) Spatially functionalized polymer surfaces
567 produced via cell-mediated lithography. *Adv. Mater.* 9, 751–755
- 568 12 Hayden, O. and Dickert, F.L. (2001) Selective microorganism detection with cell

- 569 surface imprinted polymers. *Adv. Mater.* 13, 1480–1483
- 570 13 Seiffter, A. *et al.* (2009) Synthetic receptors for selectively detecting erythrocyte ABO
571 subgroups. *Anal. Chim. Acta* 651, 215-219
- 572 14 Ren, K. *et al.* (2013) Sorting inactivated cells using cell-imprinted polymer thin films.
573 *ACS Nano* 7, 6031–6036
- 574 15 Hayden, O. *et al.* (2003) Mass-sensitive detection of cells, viruses and enzymes with
575 artificial receptors. *Sens. Actuat. B Chem*, 91, 316-319
- 576 16 Lieberzeit, P.A. *et al.* (2005) Softlithography in chemical sensing - Analytes from
577 molecules to cells. *Sensors* 5, 509-518
- 578 17 Ren, K. and Zare, R.N. (2012) Chemical recognition in cell-imprinted polymers. *ACS*
579 *Nano* 6, 4314–4318
- 580 18 Latif, U. *et al.* (2014) Biomimetic receptors for bioanalyte detection by quartz crystal
581 microbalances — from molecules to cells. *Sensors (Switzerland)* 14, 23419–23438
- 582 19 Mutreja, I. *et al.* (2015) Positive and negative bioimprinted polymeric substrates: New
583 platforms for cell culture. *Biofabrication* 7, 025002
- 584 20 Poller, A.M. *et al.* (2017) Surface Imprints: Advantageous Application of Ready2use
585 Materials for Bacterial Quartz-Crystal Microbalance Sensors. *ACS Appl. Mater.*
586 *Interfaces* 9, 1129–1135
- 587 21 Dulay, M. *et al.* (2018) Pathogen-Imprinted Organosiloxane Polymers as Selective
588 Biosensors for the Detection of Targeted E. coli. *C* 4, 29
- 589 22 Bao, H. *et al.* (2017) Bacteria-templated fabrication of a charge heterogeneous
590 polymeric interface for highly specific bacterial recognition. *Chem. Commun.* 53,

- 591 2319–2322
- 592 23 Borovička, J. *et al.* (2013) Photothermal colloid antibodies for shape-selective
593 recognition and killing of microorganisms. *J. Am. Chem. Soc.* 135, 5282–5285
- 594 24 Borovička, J. *et al.* (2013) Shape recognition of microbial cells by colloidal cell
595 imprints. *Nanoscale* 5, 8560–8568
- 596 25 Magennis, E.P. *et al.* (2014) Bacteria-instructed synthesis of polymers for self-
597 selective microbial binding and labelling. *Nat. Mater.* 13, 748–755
- 598 26 Brahmabhatt, H. *et al.* (2016) Improvement of DNA recognition through molecular
599 imprinting: Hybrid oligomer imprinted polymeric nanoparticles (oligoMIP NPs).
600 *Biomater. Sci.* 4, 281–287
- 601 27 Poma, A. *et al.* (2014) Nucleoside-tailored molecularly imprinted polymeric
602 nanoparticles (MIP NPs). *Macromolecules* 47, 6322–6330
- 603 28 Bossi, A.M. *et al.* (2012) Fingerprint-imprinted polymer: Rational selection of peptide
604 epitope templates for the determination of proteins by molecularly imprinted polymers.
605 *Anal. Chem.* 84, 4036–4041
- 606 29 Wang, S. *et al.* (2016) Targeting and Imaging of Cancer Cells via Monosaccharide-
607 Imprinted Fluorescent Nanoparticles. *Sci. Rep.* 6, 22757
- 608 30 Wang, S. *et al.* (2017) Pattern Recognition of Cells via Multiplexed Imaging with
609 Monosaccharide-Imprinted Quantum Dots. *Anal. Chem.* 89, 5646–5662
- 610 31 Liu, R. *et al.* (2017) Preparation of sialic acid-imprinted fluorescent conjugated
611 nanoparticles and their application for targeted cancer cell imaging. *ACS Appl. Mater.*
612 *Interfaces* 9, 3006–3015

- 613 32 Panagiotopoulou, M. *et al.* (2017) Fluorescent molecularly imprinted polymers as
614 plastic antibodies for selective labeling and imaging of hyaluronan and sialic acid on
615 fixed and living cells. *Biosens. Bioelectron.* 88, 85–93
- 616 33 Demir, B. *et al.* (2018) Tracking Hyaluronan: Molecularly Imprinted Polymer Coated
617 Carbon Dots for Cancer Cell Targeting and Imaging. *ACS Appl. Mater. Interfaces* 10,
618 3305–3313
- 619 34 Kinoshita, T. *et al.* (2017) Shape Memory Characteristics of O157-Antigenic Cavities
620 Generated on Nanocomposites Consisting of Copolymer-Encapsulated Gold
621 Nanoparticles. *Anal. Chem.* 89, 4680–4684
- 622 35 Piletsky, S.S. *et al.* (2017) Development of molecularly imprinted polymers specific
623 for blood antigens for application in antibody-free blood typing. *Chem. Commun.* 53,
624 1793–1796
- 625 36 El-Schich, Z. *et al.* (2016) Different expression levels of glycans on leukemic cells—a
626 novel screening method with molecularly imprinted polymers (MIP) targeting sialic
627 acid. *Tumor Biol.* 37, 13763–13768
- 628 37 Cenci, L. *et al.* (2016) Guided folding takes a start from the molecular imprinting of
629 structured epitopes. *Nanoscale* 8, 15665–15670
- 630 38 Liu, D. *et al.* (2018) Preparation of protein molecular-imprinted polysiloxane
631 membrane using calcium alginate film as matrix and its application for cell culture.
632 *Polymers (Basel)*. 10, 170.
- 633 39 Pan, G. *et al.* (2017) An Epitope-Imprinted Biointerface with Dynamic Bioactivity for
634 Modulating Cell–Biomaterial Interactions. *Angew. Chemie - Int. Ed.* 56, 15959–15963
- 635 40 Zhao, Y. *et al.* (2018) Self-assembled selenium nanoparticles and their application in

636 the rapid diagnostic detection of small cell lung cancer biomarkers. *Soft Matter* 14,
637 481–489

638 41 Wu, Z. *et al.* (2015) Preparation and evaluation of amoxicillin loaded dual molecularly
639 imprinted nanoparticles for anti-*Helicobacter pylori* therapy. *Int. J. Pharm.* 496, 1006–
640 1014

641 42 Han, J. *et al.* (2015) Preliminary investigations into surface molecularly imprinted
642 nanoparticles for *Helicobacter pylori* eradication. *Acta Pharm. Sin. B* 5, 577–582

643 43 Canfarotta, F. *et al.* (2018) Specific Drug Delivery to Cancer Cells with Double-
644 Imprinted Nanoparticles against Epidermal Growth Factor Receptor. *Nano Lett.* 18,
645 4641–4646

646 44 Bacskay, I. *et al.* (2006) Universal method for synthesis of artificial gel antibodies by
647 the imprinting approach combined with a unique electrophoresis technique for
648 detection of minute structural differences of proteins, viruses, and cells (bacteria). III:
649 Gel antibodies against . *Electrophoresis* 27, 4682–4687

650 45 Cohen, T. *et al.* (2010) Whole cell imprinting in sol-gel thin films for bacterial
651 recognition in liquids: Macromolecular fingerprinting. *Int. J. Mol. Sci.* 11, 1236–1252

652 46 Hu, Y. *et al.* (2014) Isolation of viable type I and II methanotrophs using cell-
653 imprinted polyurethane thin films. *ACS Appl. Mater. Interfaces* 6, 20550–20556

654 47 Harvey, S.D. *et al.* (2006) Preparation and evaluation of spore-specific affinity-
655 augmented bio-imprinted beads. *Anal. Bioanal. Chem.* 386, 211–219

656 48 Fukazawa, K. and Ishihara, K. (2009) Fabrication of a cell-adhesive protein imprinting
657 surface with an artificial cell membrane structure for cell capturing. *Biosens.*
658 *Bioelectron.* 25, 609–614

- 659 49 Pan, G. *et al.* (2013) Thermo-responsive hydrogel layers imprinted with RGDS
660 peptide: A system for harvesting cell sheets. *Angew. Chemie - Int. Ed.* 52, 6907–6911
- 661 50 Guilak, F. *et al.* (2009) Control of Stem Cell Fate by Physical Interactions with the
662 Extracellular Matrix. *Cell. Stem Cell.* 5, 17–26
- 663 51 Watt, F.M. and Huck, W.T.S. (2013) Role of the extracellular matrix in regulating
664 stem cell fate. *Nat. Rev. Mol. Cell Biol.* 14, 467–473
- 665 52 McMurray, R.J. *et al.* (2013) Surface topography regulates wnt signaling through
666 control of primary cilia structure in mesenchymal stem cells. *Sci. Rep.* 3, 3545
- 667 53 Mahmoudi, M. *et al.* (2013) Cell-imprinted substrates direct the fate of stem cells. *ACS*
668 *Nano* 7, 8379–8384
- 669 54 Mashinchian, O. *et al.* (2014) Cell-imprinted substrates act as an artificial niche for
670 skin regeneration. *ACS Appl. Mater. Interfaces* 6, 13280–13292
- 671 55 Bonakdar, S. *et al.* (2016) Cell-Imprinted Substrates Modulate Differentiation,
672 Redifferentiation, and Transdifferentiation. *ACS Appl. Mater. Interfaces* 8, 13777–
673 13784
- 674 56 Handgretinger, R. *et al.* (1998) Isolation and transplantation of autologous peripheral
675 CD34+ progenitor cells highly purified by magnetic-activated cell sorting. *Bone*
676 *Marrow Transplant.* 21, 987–993
- 677 57 To, L.B. *et al.* (1997) The Biology and Clinical Uses of Blood Stem Cells. *J. Am. Soc.*
678 *Hematol.* 89, 2233-2258
- 679 58 Mancardi, G. and Saccardi, R. (2008) Autologous haematopoietic stem-cell
680 transplantation in multiple sclerosis. *Lancet Neurol.* 7, 626–636

681 59 Tomlinson, M.J. *et al.* (2013) Cell separation: Terminology and practical
682 considerations. *J. Tissue Engin.* 4, 1–14

683 60 Ivanova-Mitseva, P.K. *et al.* (2012) Cubic molecularly imprinted polymer
684 nanoparticles with a fluorescent core *Angew. Chemie - Int. Ed.* 51, 5196-5199

685 61 Wang, X. *et al.* (2019) Fabrication of Core-Shell Magnetic Molecularly Imprinted
686 Nanospheres towards Hypericin via Click Polymerization. *Polymers* 11, E313

687 62 Bobo, D. *et al.* (2016) Nanoparticle-Based Medicines: A Review of FDA-Approved
688 Materials and Clinical Trials to Date. *Pharm. Res.* 33, 2373–2387

689 63 Kawabata, Y. *et al.* (2011) Formulation design for poorly water-soluble drugs based on
690 biopharmaceutics classification system: Basic approaches and practical applications.
691 *Int. J. Pharm.* 420, 1–10

692 64 Dobrovolskaia, M.A. and McNeil, S.E. (2007) Immunological properties of engineered
693 nanomaterials. *Nat. Nanotechnol.* 2, 469–78

694 65 Sun, X. *et al.* (2005) An assessment of the effects of shell cross-linked nanoparticle
695 size, core composition, and surface PEGylation on in vivo biodistribution.
696 *Biomacromolecules* 6, 2541–2554

697 66 Alexis, F. *et al.* (2008) Factors affecting the clearance and biodistribution of polymeric
698 nanoparticles. *Mol. Pharm.* 5, 505–515

699 67 Canfarotta, F. *et al.* (2016) Biocompatibility and internalization of molecularly
700 imprinted nanoparticles. *Nano Res.* 9, 3463–3477

701 68 Junginger, H. (1994) Drug absorption enhancement, concepts, possibilities, limitations
702 and trends. In *Journal of Drug Targeting* pp. 325–365

703 69 Jung, T. *et al.* (2000) Biodegradable nanoparticles for oral delivery of peptides: is there
704 a role for polymers to affect mucosal uptake? *Eur. J. Pharm. Biopharm.* 50, 147–60

705 70 Nefzger, M. *et al.* (1984) Distribution and elimination of polymethyl methacrylate
706 nanoparticles after peroral administration to rats. *J. Pharm. Sci.* 73, 1309–1311

707 71 Zhang, K. *et al.* (2016) A pH/glutathione double responsive drug delivery system
708 using molecular imprint technique for drug loading. *Appl. Surf. Sci.* 389, 1208–1213

709 72 Paul, P.K. *et al.* (2017) Improvement in insulin absorption into gastrointestinal
710 epithelial cells by using molecularly imprinted polymer nanoparticles: Microscopic
711 evaluation and ultrastructure. *Int. J. Pharm.* 530, 279–290

712 73 Mao, C. *et al.* (2017) The controlled drug release by pH-sensitive molecularly
713 imprinted nanospheres for enhanced antibacterial activity. *Mater. Sci. Eng. C* 77, 84–
714 91

715 74 Esfandyari-Manesh, M. *et al.* (2016) Paclitaxel molecularly imprinted polymer-PEG-
716 folate nanoparticles for targeting anticancer delivery: Characterization and cellular
717 cytotoxicity. *Mater. Sci. Eng. C* 62, 626–633

718 75 Da Silva, M.S. *et al.* (2011) Development of 2-(dimethylamino)ethyl methacrylate-
719 based molecular recognition devices for controlled drug delivery using supercritical
720 fluid technology. *Int. J. Pharm.* 416, 61–68

721 76 Alexis, F. *et al.* Nanoparticle technologies for cancer therapy. , *Handbook of*
722 *Experimental Pharmacology*, 197. (2010) , 55–86

723 77 Asadi, E. *et al.* (2016) Synthesis, characterization and in vivo drug delivery study of a
724 biodegradable nano-structured molecularly imprinted polymer based on cross-linker of
725 fructose. *Polymer (Guildf)*. 97, 226–237

- 726 78 Albanese, A. *et al.* (2012) The Effect of Nanoparticle Size, Shape, and Surface
727 Chemistry on Biological Systems. *Annu. Rev. Biomed. Eng.* 14, 1–16
- 728 79 Peer, D. *et al.* Nanocarriers as an emerging platform for cancer therapy. , *Nature*
729 *Nanotechnology*, 2. Dec-(2007) , 751–760
- 730 80 Liu, T. *et al.* (2019) Molecular imprinted S-nitrosothiols nanoparticles for nitric oxide
731 control release as cancer target chemotherapy. *Colloids Surfaces B Biointerfaces* 173,
732 356–365
- 733 81 Canfarotta, F. *et al.* (2018) Specific Drug Delivery to Cancer Cells with Double-
734 Imprinted Nanoparticles against Epidermal Growth Factor Receptor. *Nano Lett.* 18,
735 4641–4646
- 736 82 Ekpenyong-Akiba, A.E. *et al.* (2019) Detecting and targeting senescent cells using
737 molecularly imprinted nanoparticles. *Nanoscale Horizons* 4, 757–768
- 738 83 Pacheco, J.M. and Camidge, D.R. (2018) Antibody drug conjugates in thoracic
739 malignancies. *Lung Cancer* 124, 260–269
- 740 84 Maruani, A. (2018) Bispecifics and antibody–drug conjugates: A positive synergy.
741 *Drug Discov. Today Technol.* 30, 55–61
- 742 85 Dong, P. *et al.* (2019) Innovative nano-carriers in anticancer drug delivery-a
743 comprehensive review. *Bioorg. Chem.* 85, 325–336
- 744 86 Motib, A. *et al.* (2017) Modulation of Quorum Sensing in a Gram-Positive Pathogen
745 by Linear Molecularly Imprinted Polymers with Anti-infective Properties. *Angew.*
746 *Chemie - Int. Ed.* 56, 16555–16558
- 747 87 Long, Y. *et al.* (2016) Novel polymeric nanoparticles targeting the lipopolysaccharides
748 of *Pseudomonas aeruginosa*. *Int. J. Pharm.* 502, 232–24

- 749 88 Rechichi, A. *et al.* (2007) New biomedical devices with selective peptide recognition
750 properties. Part 1: Characterization and cytotoxicity of molecularly imprinted
751 polymers. *J. Cell. Mol. Med.* 11, 1367–1376
- 752 89 Jantarat, C. *et al.* (2008) S-Propranolol imprinted polymer nanoparticle-on-
753 microsphere composite porous cellulose membrane for the enantioselectively
754 controlled delivery of racemic propranolol. *Int. J. Pharm.* 349, 212–225
- 755 90 Destito, G. *et al.* (2007) Folic Acid-Mediated Targeting of Cowpea Mosaic Virus
756 Particles to Tumor Cells. *Chem. Biol.* 14, 1152–1162
- 757 91 Kütting, B. *et al.* (2009) Acrylamide as environmental noxious agent. A health risk
758 assessment for the general population based on the internal acrylamide burden. *Int. J.*
759 *Hyg. Environ. Health* 212, 470–480
- 760 92 Gunatillake, P.A. and Adhikari, R. (2015) Nondegradable synthetic polymers for
761 medical devices and implants. In *Biosynthetic Polymers for Medical Applications* pp.
762 33–62, Woodhead Publishing
- 763 93 Smith, L.E. *et al.* (2006) Examination of the effects of poly(N-vinylpyrrolidinone)
764 hydrogels in direct and indirect contact with cells. *Biomaterials* 27, 2806–2812
- 765 94 Lithner, D. *et al.* (2011) Environmental and health hazard ranking and assessment of
766 plastic polymers based on chemical composition. *Sci. Total Environ.* 409, 3309–3324
- 767 95 Canfarotta, F. *et al.* (2016) Solid-phase synthesis of molecularly imprinted
768 nanoparticles. *Nat. Protoc.* 11, 443–455
- 769 96 Kunath, S. *et al.* (2015) Cell and Tissue Imaging with Molecularly Imprinted Polymers
770 as Plastic Antibody Mimics. *Adv. Healthc. Mater.* 4, 1322–1326
- 771 97 Panagiotopoulou, M. *et al.* (2016) Molecularly Imprinted Polymer Coated Quantum

772 Dots for Multiplexed Cell Targeting and Imaging. *Angew. Chemie - Int. Ed.* 55, 8244–
773 8248

774 98 Cecchini, A. *et al.* (2017) In Vivo Recognition of Human Vascular Endothelial Growth
775 Factor by Molecularly Imprinted Polymers. *Nano Lett.* 17, 2307–2312

776 99 Mori, T. and Katayama, Y. (2019) Signal amplification in flow cytometry for cell
777 surface antigen analysis. *J. Biochem.* 166, 205–212

778 100 Skottrup, P.D. *et al.* (2008) Towards on-site pathogen detection using antibody-based
779 sensors. *Biosens. Bioelectron.* 24, 339–348

780 101 Tokonami, S. *et al.* (2014) Recognition of gram-negative and gram-positive bacteria
781 with a functionalized conducting polymer film. *Research on Chemical Intermediates*
782 40, 2327–2335

783 102 Spieker, E. and Lieberzeit, P.A. (2016) , Molecular Imprinting Studies for Developing
784 QCM-sensors for Bacillus Cereus. , in *Procedia Engineering*, 168, pp. 561–564

785 103 Schnettelker, A. and Lieberzeit, P. (2016) , A Self-Organisation Synthesis Approach
786 for Bacteria Molecularly Imprinted Polymers. *Procedia Engineering*, 168, pp. 557–
787 560

788 104 Yilmaz, E. *et al.* (2015) Whole cell imprinting based Escherichia coli sensors: A study
789 for SPR and QCM. *Sensors Actuators, B Chem.* 209, 714–721

790 105 Seidler, K. *et al.* (2009) Biomimetic yeast cell typing - Application of QCMs. *Sensors*
791 9, 8146–8157

792 106 Samardzic, R. *et al.* (2014) Quartz Crystal Microbalance In-Line Sensing of
793 Escherichia Coli in a Bioreactor Using Molecularly Imprinted Polymers. *Sens. Lett.*
794 12, 1152–1155

795 107 Khan, M.A.R. *et al.* (2016) Plastic antibody for the electrochemical detection of
796 bacterial surface proteins. *Sensors Actuators, B Chem.* 233, 697–704

797 108 Golabi, M. *et al.* (2017) Electrochemical bacterial detection using poly(3-
798 aminophenylboronic acid)-based imprinted polymer. *Biosens. Bioelectron.* 93, 87–93

799 109 Namvar, A. and Warriner, K. (2007) Microbial imprinted polypyrrole/poly(3-
800 methylthiophene) composite films for the detection of *Bacillus endospores*. *Biosens.*
801 *Bioelectron.* 22, 2018–2024

802 110 Liang, R. *et al.* (2017) Mussel-Inspired Surface-Imprinted Sensors for Potentiometric
803 Label-Free Detection of Biological Species. *Angew. Chemie - Int. Ed.* 56, 6833–6837

804 111 Idil, N. *et al.* (2017) Whole cell based microcontact imprinted capacitive biosensor for
805 the detection of *Escherichia coli*. *Biosens. Bioelectron.* 87, 807–815

806 112 Qi, P. *et al.* (2013) Impedimetric biosensor based on cell-mediated bioimprinted films
807 for bacterial detection. *Biosens. Bioelectron.* 39, 282–288

808 113 Zhang, Z. *et al.* (2015) Highly stable and reusable imprinted artificial antibody used
809 for in situ detection and disinfection of pathogens. *Chem. Sci.* 6, 2822–2826

810 114 Chen, S. *et al.* (2017) Electrochemiluminescence Detection of *Escherichia coli*
811 O157:H7 Based on a Novel Polydopamine Surface Imprinted Polymer Biosensor. *ACS*
812 *Appl. Mater. Interfaces* 9, 5430–5436

813 115 Steen Redeker, E. *et al.* (2017) Biomimetic Bacterial Identification Platform Based on
814 Thermal Wave Transport Analysis (TWTA) through Surface-Imprinted Polymers. *ACS*
815 *Infect. Dis.* 3, 388–397

816 116 Van Grinsven, B. *et al.* (2014) The heat-transfer method: A versatile low-cost, label-
817 free, fast, and user-friendly readout platform for biosensor applications. *ACS Appl.*

818 *Mater. Interfaces* 6, 13309–13318

819 117 Eersels, K. *et al.* (2015) Improving the sensitivity of the heat-transfer method (HTM)
820 for cancer cell detection with optimized sensor chips. *Phys. Status Solidi Appl. Mater.*
821 *Sci.* 212, 1320–1326

822 118 Eersels, K. *et al.* (2013) Selective identification of macrophages and cancer cells based
823 on thermal transport through surface-imprinted polymer layers. *ACS Appl. Mater.*
824 *Interfaces* 5, 7258–7267

825 119 Jenik, M. *et al.* (2009) Sensors for bioanalytes by imprinting-Polymers mimicking both
826 biological receptors and the corresponding bioparticles. *Biosens. Bioelectron.* 25, 9–14

827 120 Dong, Y. *et al.* (2019) Inhibition of HER2-Positive Breast Cancer Growth by Blocking
828 the HER2 Signaling Pathway with HER2-Glycan-Imprinted Nanoparticles. *Angew.*
829 *Chemie - Int. Ed.* 58,10621–10625

830 121 Dickert, F.L. *et al.* (2001) Synthetic receptors as sensor coatings for molecules and
831 living cells. *Analyst* 126, 766–771

832 122 Dickert, F.L. and Hayden, o. (2002) Bioimprinting of polymers and sol-gel phases.
833 Selective detection of yeasts with imprinted polymers. *Anal. Chem.* 74, 1302–1306

834 123 Xu, D. (2012) Protein Databases on the Internet. *Curr Protoc Mol Biol.* Chapter
835 19:Unit 19.4.

836 124 Henikoff, S. (1996) Scores for sequence searches and alignments. *Curr Opin Struct*
837 *Biol.* 6, 353-360

838 125 J. Xu *et al.* (2019) Molecularly Imprinted Polymer Nanoparticles as Potential
839 Synthetic Antibodies for Immunoprotection against HIV. *ACS Appl. Mater. Interfaces*
840 11, 9824-9831

- 841 126 Shan, X. *et al.* (2017) Spontaneous and specific binding of enterohemorrhagic
842 Escherichia coli to overoxidized polypyrrole-coated microspheres. *Chem. Commun.*
843 53, 3890–3893
- 844 127 SHAN, X. *et al.* (2018) Binding Constant of the Cell-shaped Cavity Formed on a
845 Polymer for Escherichia coli O157. *Anal. Sci.* 34, 483–486
- 846 128 Shan, X. *et al.* (2018) A rapid and specific bacterial detection method based on cell-
847 imprinted microplates. *Analyst* 143, 1568–1574
- 848 129 Tokonami, S. *et al.* (2013) Label-free and selective bacteria detection using a film with
849 transferred bacterial configuration. *Anal. Chem.* 85, 4925–4929
- 850 130 Tokonami, S. *et al.* (2017) Mechanism in External Field-mediated Trapping of
851 Bacteria Sensitive to Nanoscale Surface Chemical Structure. *Sci. Rep.* 7, 16651
- 852 131 Abadi, P.P.S.S. *et al.* (2018) Engineering of Mature Human Induced Pluripotent Stem
853 Cell-Derived Cardiomyocytes Using Substrates with Multiscale Topography. *Adv.*
854 *Funct. Mater.* 28, 1707378
- 855 132 Evans, J. *et al.* (2015) The characteristics of Ishikawa endometrial cancer cells are
856 modified by substrate topography with cell-like features and the polymer surface. *Int.*
857 *J. Nanomedicine* 10, 4883
- 858 133 Murray, L.M. *et al.* (2014) Bioimprinted polymer platforms for cell culture using soft
859 lithography. *J. Nanobiotechnology* 12, 60
- 860 134 Boffa, V. *et al.* (2012) Sol-gel synthesis of a biotemplated inorganic photocatalyst: A
861 simple experiment for introducing undergraduate students to materials chemistry. *J.*
862 *Chem. Educ.* 89, 1466–1469
- 863 135 Lee, M.H. *et al.* (2014) Recognition of algae by microcontact-imprinted polymers

864 modulates hydrogenase expression. *RSC Adv.* 4, 61557–61563

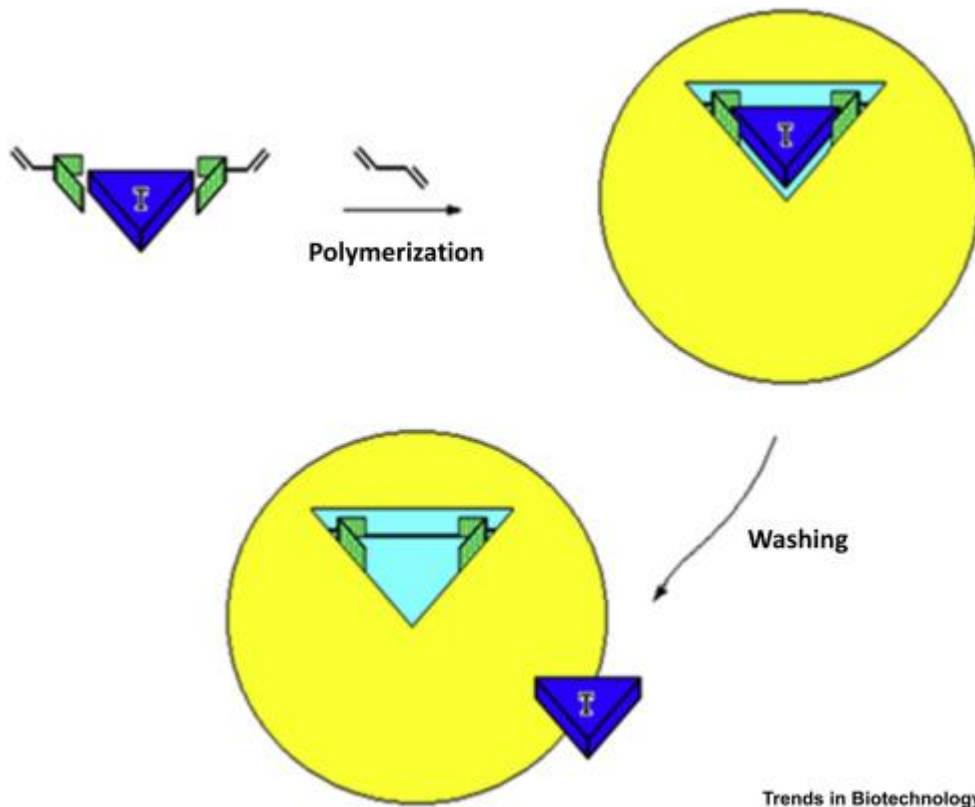
865 136 Lee, M.H. *et al.* (2014) Microcontact imprinting of algae for biofuel systems: The

866 effects of the polymer concentration. *Langmuir* 30, 14014–14020

867

868

869 **Legend to Figures**

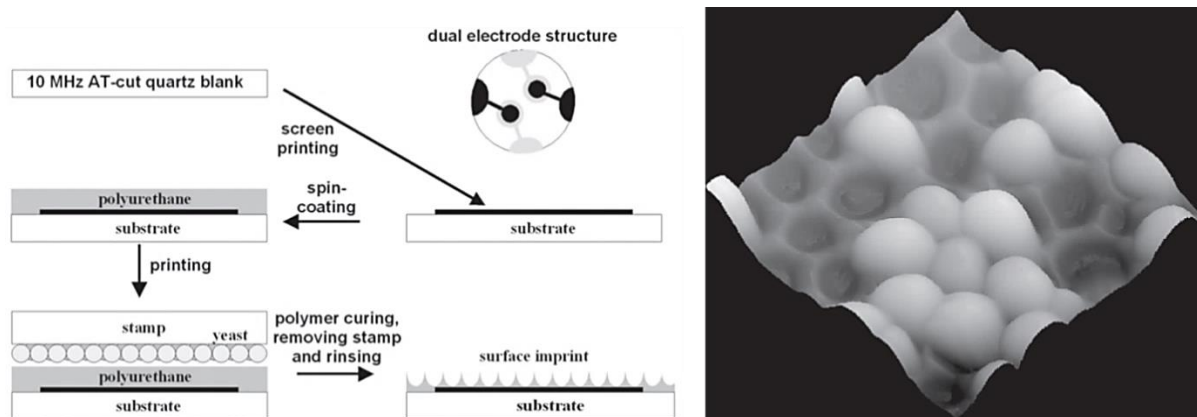


870

871 Figure 1. Schematic of the concept of the molecular imprinting. The template (blue triangle)
872 and the functional monomers (green) interact in solution forming a pre-polymerization
873 complex. The addition of the crosslinker and of the initiators yield to the synthesis of the
874 molecularly imprinted polymer (MIP; yellow). At the completion of the process, the template
875 is removed from the MIP by washing steps. The stamped recognition cavities are
876 complementary to the template and ready for its binding.

877

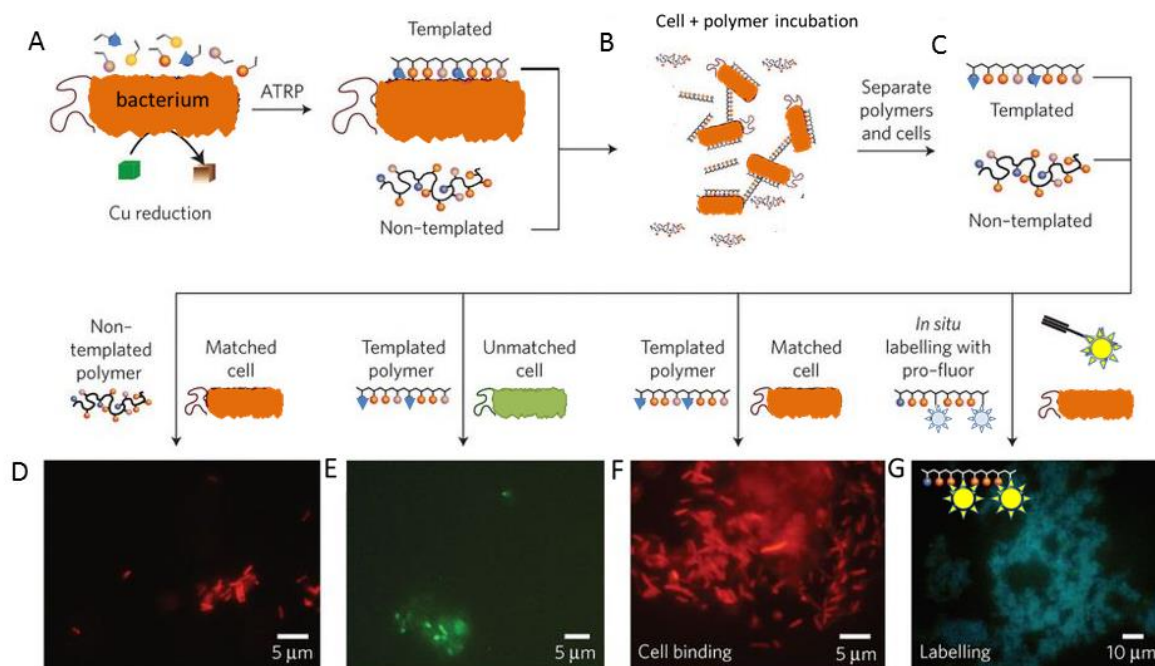
Trends in Biotechnology



878

879 Figure 2. Process of microprinting. As an example yeast cells were imprinted with PU matrix
 880 [12,121]. As typical for micro-contact stamping, a stamp containing the microorganisms (made
 881 by preparing a “sandwich” of cells between glass and Teflon) was pressed into a prepolymer
 882 mixture which was then cured, with the resulting cavities exhibited hexagonal, honeycomb-
 883 like packing [122]. Left - the surface of quartz crystal is coated with pre-polymerized
 884 polyurethane and stamped with immobilised *S. cerevisiae*, creating imprints capable of re-
 885 binding of template species. Right - a tapping mode AFM image of the imprinted polyurethane
 886 layer after exposition to a *S. cerevisiae* solution. Reprinted with permission from [12].

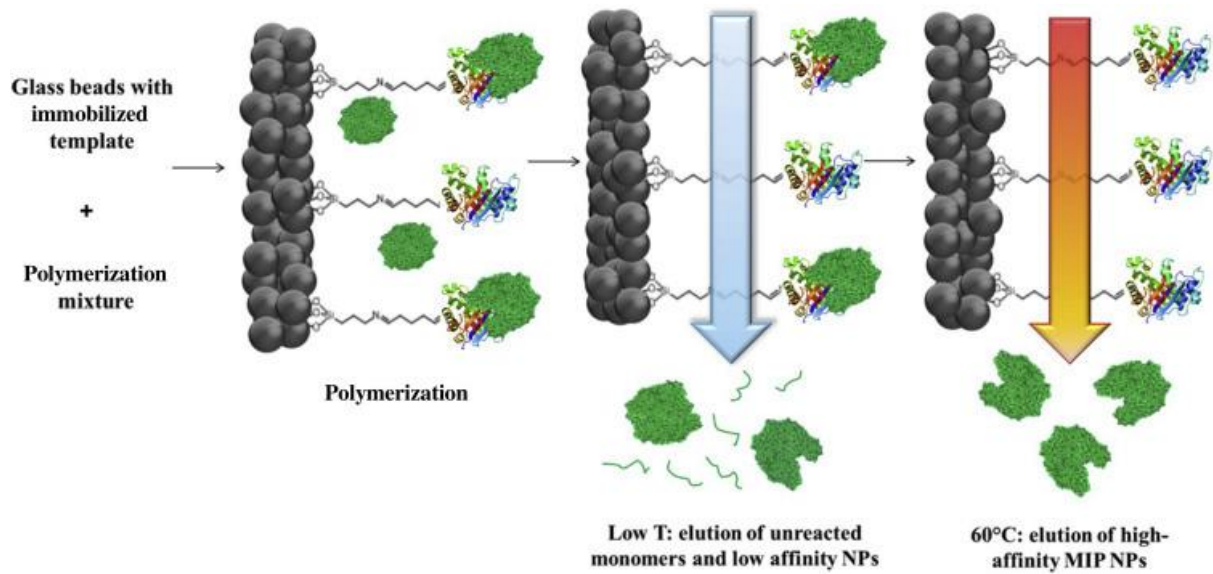
887



888

889 Figure 3. (A,B) Bacteria induce polymerization in monomer suspensions to generate MIPs. (C)
 890 Polymers are recovered from the suspensions to generate templated and nontemplated
 891 fractions. (D) Incubation of polymers with bacteria results in low binding of cells to
 892 nontemplated MIPs or (E) where a polymer templated with one cell type (shown in orange) is
 893 incubated with a cell (shown in green) of another type. (F) Addition of a polymer, templated
 894 by one cell type, with its own 'matched' cell population results in the formation of large
 895 polymer-cell clusters. (G) Labeling the cells *in situ* via pro-fluorescent markers, which react
 896 with cell surface-bound polymers containing 'clickable' residues. Adapted, with permission,
 897 from [25].

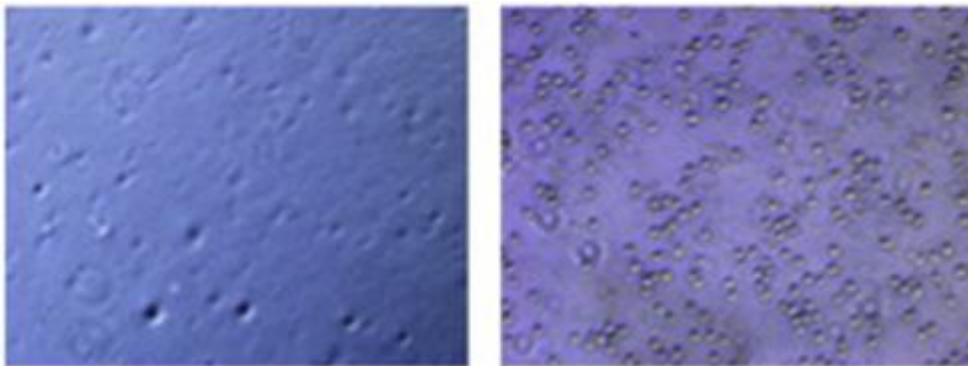
898



899

900 Figure 4. Schematic Representation of the Automated Synthesis of Nanoscale Molecularly
 901 Imprinted Polymers (NanoMIPs) Using an Immobilized Template (Melamine) [8].
 902 Abbreviation: NP, nanoparticle.

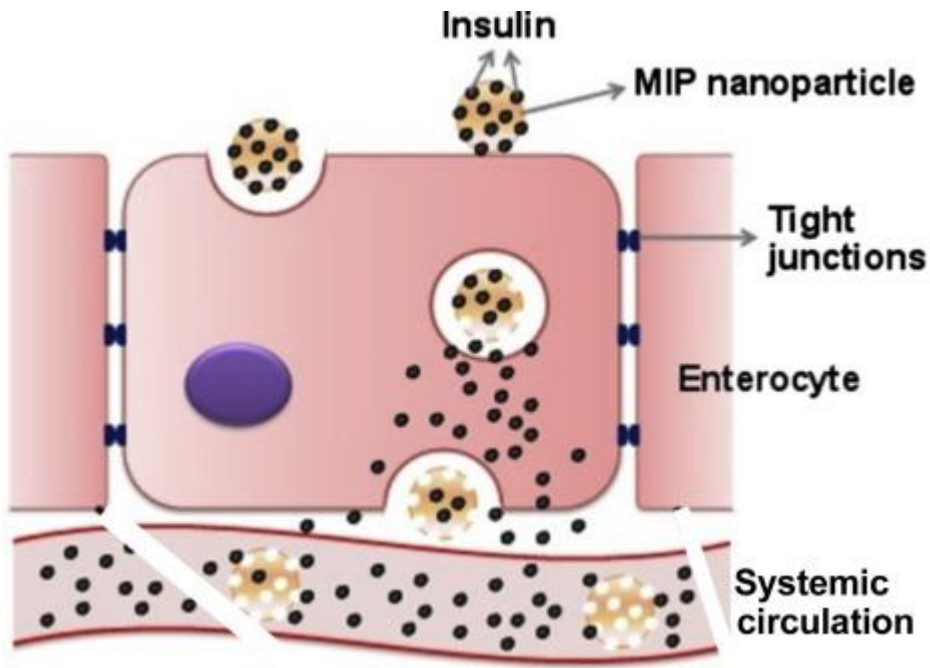
903



904

905 Figure 5. L929 cell adhesion on BSA (left) and FN-imprinted (right) substrates. Reprinted
 906 with permission from [48].

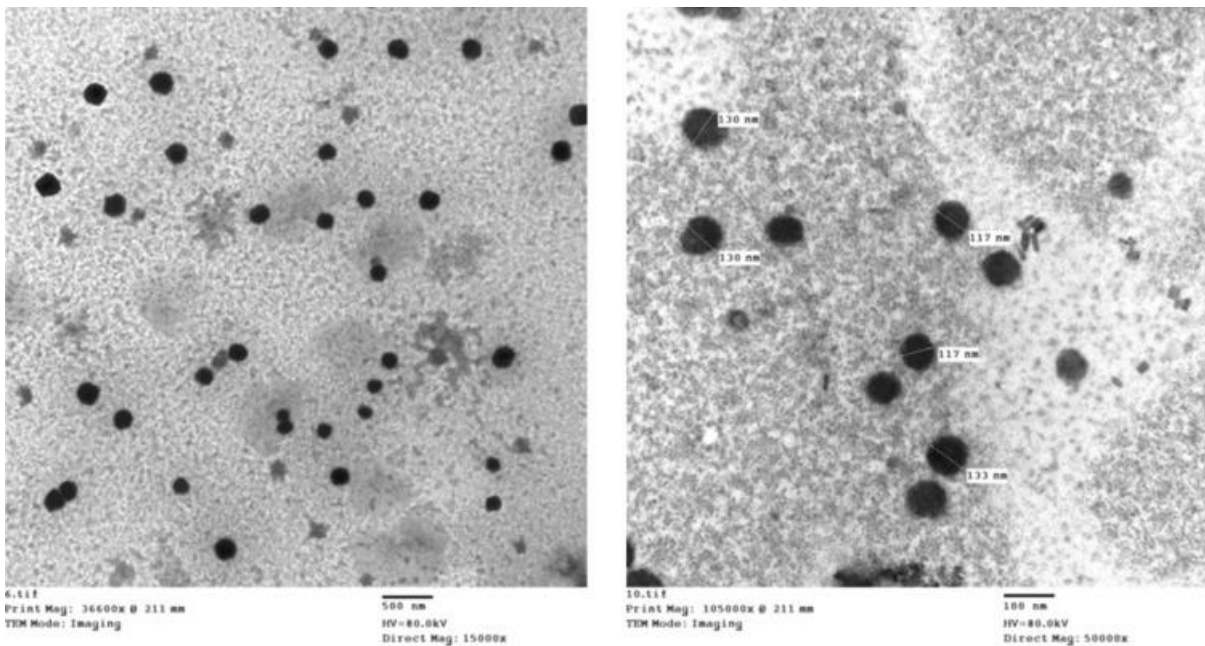
907



908

909 Figure 6. Schematic of the Transport of Insulin-Loaded Molecularly Imprinted Polymer (MIP)
 910 Nanoparticles across Intestinal Epithelial Cells Following Oral Administration and Insulin
 911 Release by Endocytosis and Transcytosis through Enterocytes. Reprinted with permission from
 912 [72].

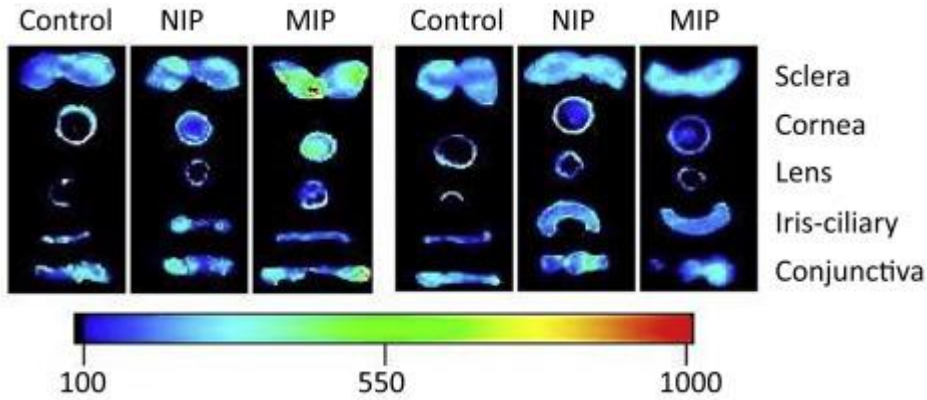
913



914

915 Figure 7 Representative Illustration of Nanoparticles (NPs) Detected in Urine by Scanning
916 Electron Microscopy (SEM). NPs were prepared by the solid phase approach using
917 vancomycin as a template..

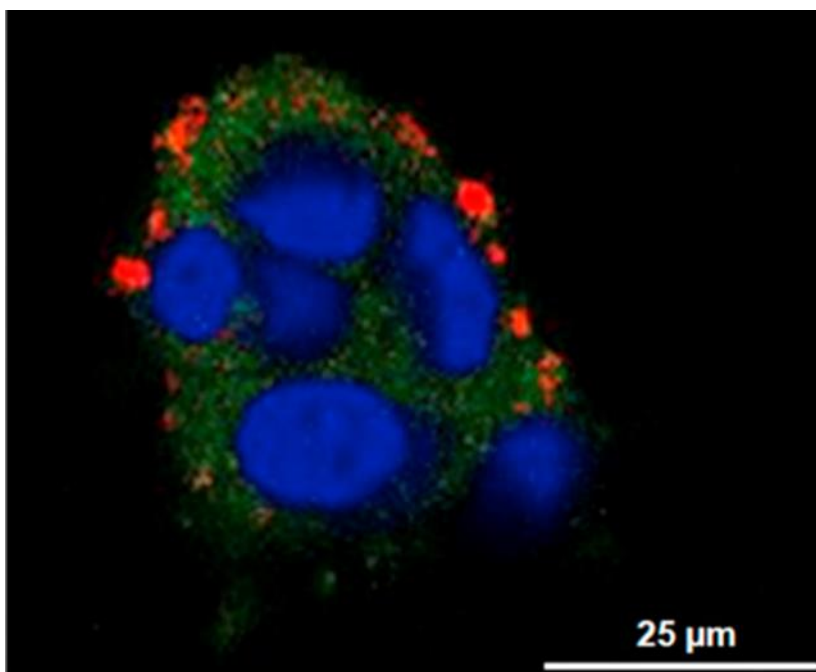
918



919

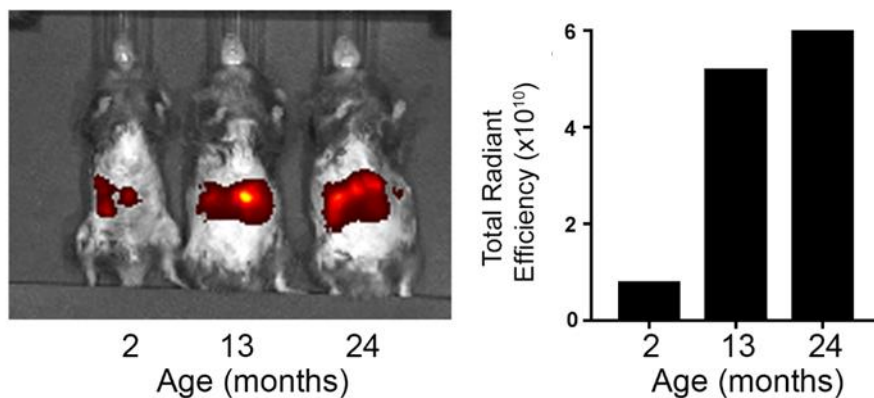
920 Figure 8. Fluorescence imaging of rabbit eye tissues taken from the keratitis model rabbits
921 (left) or normal rabbits (right), following treatment with IR-783-loaded molecularly imprinted
922 (MIP) and non-imprinted (NIP) nanoparticles. The control was treated with IR-783 solution
923 alone. Reprinted with permission from [87].

924



925

926 Figure 9. Confocal Image Showing Simultaneous Multiplex Labeling of D-Glucuronic Acid
927 (GlcA) and N-Acetylneuraminic Acid (NANA) on Fixed Human Keratinocytes by Molecularly
928 Imprinted Polymer (MIP) GlcA Quantum Dots (QDs) (MIPGlcA-QDs, Green) and
929 MIPNANA-QDs (red), respectively.. Reprinted with permission from [32].
930



931
932 Figure 10. Representative images of group of mice of different ages, injected intravenously
933 with Alexa Fluor 647-tagged B2M Nanoscale Molecularly Imprinted Polymers (nanoMIPs).
934 Animals were imaged 2 h after injection. Total fluorescence signals were quantified and are
935 shown in units of radiant efficiency. Reprinted, with permission, from [82].

936 **BOX 1**

937 **Rational selection of linear epitope templates**

938 *When to use & which bioinformatics resources are available:* A peptide can be a “signature”
939 for the whole protein. Such a peptide, called idiotypic, or unique, is envisaged as ideal target
940 for the imprinting. Beside the cost-associated considerations, the imprinting of a small portion
941 of the protein bypasses all the problems associated with unfolding during the imprinting
942 process, enabling to provide a material with imprinted stereochemical images for the target
943 peptide. The selection of a signature peptide from a protein is enabled by the access to free
944 web-curated repositories of proteomics information, i.e. the websites where all the known
945 protein sequences are stored (e.g. NCBI, UniProt) [123].

946 The goal to find a unique peptide sequence within the targeted protein can be fulfilled thanks
947 to the sequence alignment of comparison tools provided by the database. Once the sequence
948 comparison query is submitted, the query is replied by a report in which a scoring system gives
949 the measure to the goodness of the alignment between the compared sequences [124],
950 consequently the selection of the unique peptide has been named “rational” to indicate that
951 objective goodness criteria are applied in form of a score [28]. The steps for the identification
952 of the epitope are: the target protein sequence is selected, cut *in silico* into peptides by choosing
953 a suitable cutting agent (e.g. trypsin); too small peptides are discarded (these are considered
954 too combinations that can be found with high frequency, thus not good to mark uniqueness),
955 whereas peptides of significant length (8-15 aminoacids) are aligned to the whole protein
956 sequences database. The best peptide epitope is the one that aligned towards the whole database
957 of protein sequences provides the best match (highest score; S) for the very parental protein,
958 while having the lowest E-value (value indicating the number for distinct alignments, with a
959 score equivalent to or better than S, but expected to occur in a database search by chance).

960

961 **1. From the website <http://www.uniprot.org/>**

- 962 • search for the target protein sequence ; copy the sequence in FASTA canonical format

963 **2. From the website http://web.expasy.org/peptide_cutter/**

- 964 • paste the FASTA sequence in the appropriate box ;
- 965 • select the desired cleavage method (enzymes, chemicals) ; select “Table of sites, sorted
- 966 sequentially by amino acid number” and cleave the protein;
- 967 • select peptides not shorter than 8-10 (idiotypic sequences) and not longer than 15
- 968 residues (avoid secondary structures);

969 **3. From the site <http://blast.ncbi.nlm.nih.gov/Blast.cgi> and select “protein blast”**

- 970 • enter one by one the sequences of the selected peptides in the appropriate box and set
- 971 the following parameters before running:

972 * Database: non-redundant protein sequences (nr) ; * Organism: e.g. Homo sapiens ; *

973 Algorithm: blastp (protein-protein BLAST)

- 974 • report the found identity value, the total score and the E-value of each peptide; choose
- 975 the peptide with the highest total score and the lowest E-value

976 **4. From the website <http://web.expasy.org/protparam/>**

- 977 • Enter the sequence of the selected peptide/peptides in the appropriate box to calculate
- 978 the parameters: molecular weight, isoelectric point, number of negatively and positively
- 979 charged residues, GRAVY index.

980 **BOX 2**

981 **Rational selection of structured epitopes as template**

982 *When to use & which bioinformatics resources are available:* When the target protein is
983 exposed at the cell surface, the epitope might be protruding out of the membrane in fixed and
984 defined orientation, or when peptides associated with high scores are not accessible for binding,
985 because they are hidden in the protein core, masked by membrane or associated to other
986 proteins and glycocomponents.

987 The positioning of the chosen epitope on the protein 3D structure is a prerequisite for successful
988 imprint. Moreover, using directional peptides (e.g. circular peptides) instead of linear ones is
989 another strategy to ultimately gain in MIP selectivity [37, 125]. Database's tools associated
990 with 3D view of proteins permit to define the epitope localization in the protein structure.
991 Experimental, literature and predicted information gathered by and available in protein-protein
992 interaction databases (see for example: <http://string-db.org>; <https://www.ebi.ac.uk/intact/>)
993 permit to finalize the selection of the epitope restricting to the one accessible to the surface
994 (and prone for binding) and to these not involved in functional association to other proteins or
995 glycol-partners.

996

997 **1. From the website <http://www.uniprot.org/>**

- 998
- Search the target protein sequence identification number (ID)

999 **2. From the website <http://uniprot.org/uniprot/> Add appropriate ID /protvista**

- 1000
- Enter the Uniprot ID of the target protein in the Uniprot database;

1001 In the Display click on Feature viewer then select peptides by using the following two options:

1002 (A) On Structural features; Turn

1003 • Select a turn and click on it to view its location on the 3D structure

1004 • Identify the tryptic peptide that contains the desired turn by clicking on Proteomics and
1005 on the Unique peptide sequence.

1006 (B) On Antigenic sequences

1007 • Select an antibody binding sequence among those marked on the sequence of the target
1008 protein

1009 • Define a unique tryptic peptide within the antigenic sequence clicking on Proteomics
1010 and on the Unique peptide sequence.

1011

1012

Table 1. List of materials stamped by microcontact printing technique and their uses

Type of cell	Biological imprinted target	Material used	Application	Key observations	Reference
Bacteria	E. Coli	Gold-coated microbeads with Nafion + polypyrrole (PPy) imprinted layer	Cell sorting; sensing	E. Coli-shaped cavity to be $1.1 \times 10^5 \text{ M}^{-1}$; discrimination of <i>E. coli</i> , <i>Acinetobacter calcoaceticus</i> and <i>Serratia marcescens</i>	126, 127, 128
		Polypyrrole (PPY)	Sensor; Quartz crystal microbalance (QCM)	discrimination of <i>E. coli</i> , <i>Pseudomonas aeruginosa</i> , <i>Bacillus subtilis</i> , <i>Staphylococcus aureus</i> , <i>A. calcoaceticus</i> and <i>S. marcescens</i>	101,129
		Polypyrrole (PPY)	Sensor; QCM for food poisoning detection	discrimination of <i>E. coli</i> O157:H7, <i>Salmonella enterica</i> , <i>Vibrio parahaemolyticus</i> , <i>S. aureus</i>	130
Mammalian cells	Cardiomyocytes	Polydimethylsiloxane (PDMS)	Cell differentiation	The MIP drives the differentiation of pluripotent cells into the desired specific subtypes	131
	Ishikawa endometrial adenocarcinoma cells	Polymethacrylate and Polystyrene (PS)	Cell culturing Cancer development mechanisms	Cells grown on imprinted surfaces expressed more adhesion proteins.	18,19,132, 133
Yeast	yeast cells	Polyurethane (PU)	Proof of principle QCM and optical sensors	PU MIPs proved sensitive coatings to planar waveguides and mass-sensitive devices for the selective detection of various microorganisms	12, 121
		Sol-gel	Proof of principle of cell discrimination	Discriminate between different strains of yeast; little or no non-specific binding taking place	134
Algae	algae	Poly(ethylene-co-vinyl alcohol)	Cell culturing Biofuel/cell	the imprinted matrix improved the overall energy production, proving the mechanical/physical effect of the topographical environment on the metabolism/growth of the cells	135, 136

1013

1014

1015
1016
1017
1018
1019
1020
1021
1022
1023
1024
1025
1026
1027
1028
1029
1030
1031
1032
1033
1034
1035
1036
1037
1038
1039
1040
1041
1042
1043
1044
1045
1046
1047
1048
1049
1050
1051
1052
1053
1054
1055
1056

Glossary

Atom transfer radical polymerisation (ATRP): it is a reversible-deactivation radical polymerization suitable for forming carbon-carbon bonds with a transition metal catalyst. ATRP permits a high degree of control of the composition and of the architecture of macromolecules, ultimately providing polymeric materials with highly specific and uniform characteristics.

Electrochemical sensor: according to IUPAC definition and classification, is a category of chemical sensors, designed by coupling the receptor part of the device to an electrochemical transducer. The transducer transforms the analytical information originating from the electrochemical interaction analyte-electrode into a measurable electrical signal.

Electrochemiluminescence biosensor: it is a biosensor that measures the emission of visible light as the result of an electrochemical reaction. Electro-chemiluminescent molecules, after becoming electronically excited, release visible electromagnetic energy when returning to their relaxed state. In the biosensor, the light-emitting molecules that interact with the analyte of interest are introduced into the solution, the amount of emitted light is measured and correlated to the quantity of analyte present in the sample.

Electropolymerization: it is the polymerization of electroactive monomers under the influence of an electric current. The method is straightforward to obtain polymer films with a certain thickness by controlling the number of cycles or the current that is applied to the electrode.

Epitope: known as antigenic determinant, it is the part of an antigen that is recognized by the immune system.

Idiotypic peptide: is a molecular arrangement of amino acids unique to the antigen-binding site of a particular antibody. The molecular structure and conformation of an antibody that confers its antigenic specificity.

Microcontact printing: is a method of transferring patterns of various materials such as polymers, proteins, nanoparticles, etc., onto another surface. Typically a polydimethylsiloxane (PDMS) stamp is dipped in a solution of a material that has to be patterned and is brought into contact with the surface. Transfer of micrometer (μm)/nanometer (nm)-size patterns is possible by this technique.

Quartz crystal microbalance (QCM) sensor: called also acoustic sensor, or quartz crystal microbalance. It is based on a piezoelectric material, or quartz crystal resonator, to which a frequency is applied. Usually the receptor, i.e. the selective MIP, is deposited on the surface of the quartz crystal resonator. The QCM measures the mass variation per unit area by measuring the change in frequency of the quartz crystal resonator. The resonance is perturbed by the addition or removal of an analyte at the surface of the acoustic resonator.